



Monte Carlo Simulations of Test Beam 21 at the DESY-II Test Beam Facility

Friederike Jöhlinger, University of Glasgow, United Kingdom

September 8, 2015

Abstract

The DESY-II test beam is mainly used by researcher teams developing detectors for testing sensors under realistic circumstances. A good understanding of the properties of the test beam is therefore essential. Multiple Monte Carlo simulations were performed using the simulation tool Simulator for the Linear Collider (SLIC) to further understanding of important operational parameters of the test beam. First neutron fluxes in the DESY-II tunnel as a result of the test beam generation were studied using two different SLIC physics lists. Additional simulations were carried out to find out more about the influence of different secondary targets on the final beam. The results were compared to experimental data. Overall a good agreement could be found between experiment and simulations.

Contents

1	Introduction	3
2	Theory	4
2.1	Test beam set-up	4
2.2	Particle interactions	5
2.2.1	Bremsstrahlung	5
2.2.2	Pair production	5
2.2.3	Other relevant interactions	5
3	Method	6
3.1	Neutron production in shielding material	7
3.2	Energy distribution of the final Test Beam using different converter plates	7
4	Results and discussion	7
4.1	Neutron Fluxes	7
4.2	Photon conversion efficiencies	9
5	Conclusions	11

1 Introduction

The DESY-II Test Beam Facility provides high energy electron and positron beams and is used to test detectors under realistic circumstances. To get a better understanding of the propagation of particles through the test beam set-up and the composition of the final beam, simulations can be performed. Simulations provide information about the progression of the primary particles, the creation of new particles in the different materials present in the test beam set-up and the properties of such secondary particles. Knowledge about the beam attributes is crucial to users testing and calibrating new detectors. It will be easier to adjust the beam to specific requirements, with a better understanding of how different parts of the test beam area influence the final beam.

A general simulation of Test Beam 21 has been performed using the Simulator for the Linear Collider (SLIC).[1] Based on the technique used for that simulation, several more specific simulations were performed. In the previous simulation it was discovered that neutron fluxes are created in the shielding material. To find out more about the origin and energy of these neutrons, the production of neutrons in the shielding materials was studied by performing simulations for the first part of the test beam set-up.

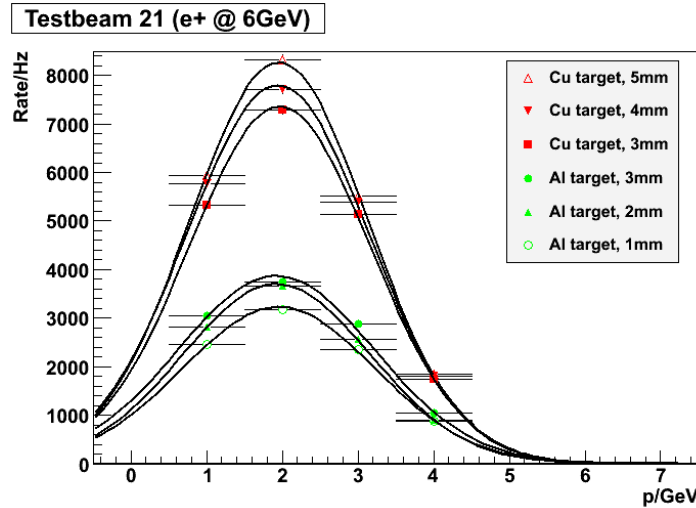


Figure 1: Rate of particles in final beam as a function of particle momentum. The original beam used to produce the bremsstrahlung is a positron beam with one bunch of about 7×10^9 particles at 6.3 GeV. [2]

After that the influence of using different converter plates on the final test beam was tested, performing multiple simulations for each converter plate. The converters used in the simulation were plates made of copper, 3 mm thick, and aluminium, 3 mm thick. Additionally, data from the previous simulation for the copper target of 5 mm were used. The results of these simulations were compared with experimental results from the final test beam, which can be seen in figure 1. From experimental data it could be concluded that the copper converter plates generate the highest rates of final particles and that

the thicker converter plates produce higher rates than the thinner ones. It is expected that the simulations will reproduce this trend.

2 Theory

2.1 Test beam set-up

The DESY-II beam is a pre-accelerator for the PETRA III ring. When DESY-II runs in top-up mode for PETRA-III, the test beams are operated simultaneously. The test beam facility consists of the beam lines 21, 22 and 24 and provides electron and positron beams of 1 to 6.3 GeV.

To produce a test beam, a carbon fibre bundle is positioned in the main DESY-II beam. When an electron bunch of the DESY-II beam hits the carbon fibres, bremsstrahlung is produced which propagates linearly, while the main beam is bent along its circular path in the magnetic field of the dipole magnets of the synchrotron ring optics. The linearly propagating photon beam then hits a converter target, producing electron-positron pairs. Using a dipole magnet the electron-positron beam is spread out under the influence of Lorentz force. The deflection of each particle in the magnetic field is dependent on the respective mass and energy. Directly after the magnet the beam pipe has a kink, so only particles propagating at a certain angle to the z-axis, the original direction of propagation, will continue on the beam line after the magnet. Therefore the particles with the required energy can be selected by varying the magnetic field. The test beam is collimated both horizontally and vertically before entering the test beam area. In the test beam area there is one final collimation before the detector location is reached. A schematic description of this process can be seen in figure 2.[1]

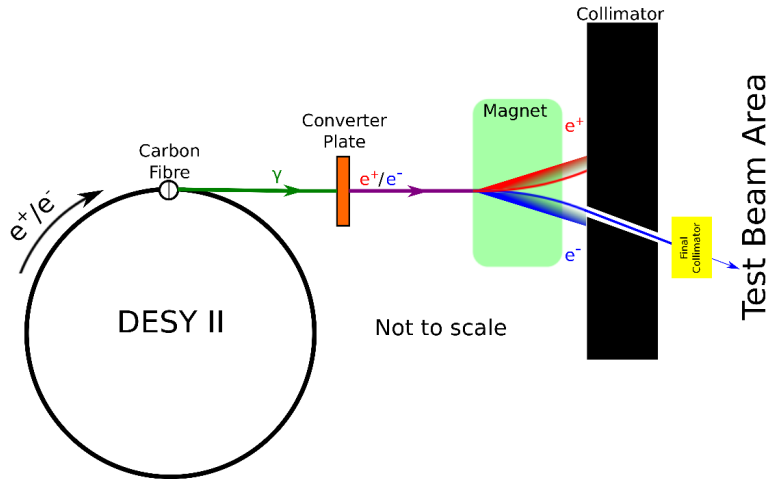


Figure 2: Overview of the DESY-II Test Beam generation

2.2 Particle interactions

Many particle interactions should be considered when simulating the test beam. Two processes are most significant: the production of bremsstrahlung by electrons in the primary beam and pair production by high energy photons in the converter targets. Further processes should not be forgotten either, as other secondary particle productions can result in significant beam losses and cause radiation damage. [3]

2.2.1 Bremsstrahlung

Bremsstrahlung is the radiation that is produced by high energy charged particles when accelerating in the field of another charged particle, for example when an electron is deflected by a nucleus. The radiation is produced tangential to the path of propagation of the deflected charged particles. At the energies considered, it is the dominant interaction mechanism of electrons with matter. Bremsstrahlung is produced in a continuous spectrum, with the maximum energy of the photons produced dependent on the energy of the deflected particle. Therefore, the electron beam in DESY-II at 6.3 GeV can produce photons with energies up to 6.3 GeV.

2.2.2 Pair production

When the energy of a photon exceeds the combined rest mass of an electron and a positron, 1.02 MeV, the photon can produce an electron-positron pair during an interaction with a nucleus. The energy of the photon is transferred to the electron and the positron while the nucleus ensures that momentum conservation is not violated. At high energies pair production is the main interaction process between photons and matter. The energy distribution between the produced electron and positron is random, with an equal division of energy between the two resulting particles being the average.

2.2.3 Other relevant interactions

For high energy photon beams, the dominant interaction with matter is pair production. However, there are more particle interactions to be considered, such as multiple scattering, the photoelectric effect and giant resonances. In the first case, particles, for example photons or electrons, interact with matter in several elastic and inelastic processes. The particles lose energy during these interactions and are deflected from their original direction of propagation. One such scattering process is Compton scattering. During this interaction electrons or other charged particle recoil in an inelastic scattering process with a photon. The photon loses energy and is scattered through a certain angle. If the photon has more energy than the binding energy of an electron in its shell, the electron can absorb the photon and be ejected from the atom. This is the so-called photoelectric effect.

Another option is the giant resonance of nuclei.[4] In this process a nucleus absorbs a photon with an energy of the order 10 MeV, enough to excite the nucleus. There is a resonant behaviour for a certain photon energy at which a nucleus absorbs photons

most readily. This resonant peak energy value is dependent on the composition of the nucleus. By the creation of a virtual particle, high energy electrons can interact with nuclei similarly, provided that the electron has an energy higher than 50 MeV. One of the processes that can occur during de-excitation, is the ejection of a particle by the nucleus. This way giant resonances can result in neutron emission in the test beam set-up.

3 Method

The test beam creation starts at the primary target, a carbon fibre bundle, in the DESY-II beam. The carbon fibres are $25\ \mu\text{m}$ thick and the beam, consisting of one bunch of 10^{10} electrons or positrons with an average energy of 6.3 GeV, circulates around the storage ring with a frequency of 1 MHz. A new bunch is injected every 160 ms and dumped after roughly 163000 turns. Every few minutes there is extraction to PETRA-II for several seconds. Furthermore there is a transverse motion of the beam of some mm.[5] All these properties together result in a significantly lower frequency of the electron bunch hitting the carbon fibre than 1MHz.

For the Monte Carlo simulations the simulation package Simulator for the Linear Collider (SLIC) was used.[6] SLIC employs the simulation toolkit Geant4 to simulate the passage of particles through a detector. In this case not a detector, but the test beam geometry was simulated.

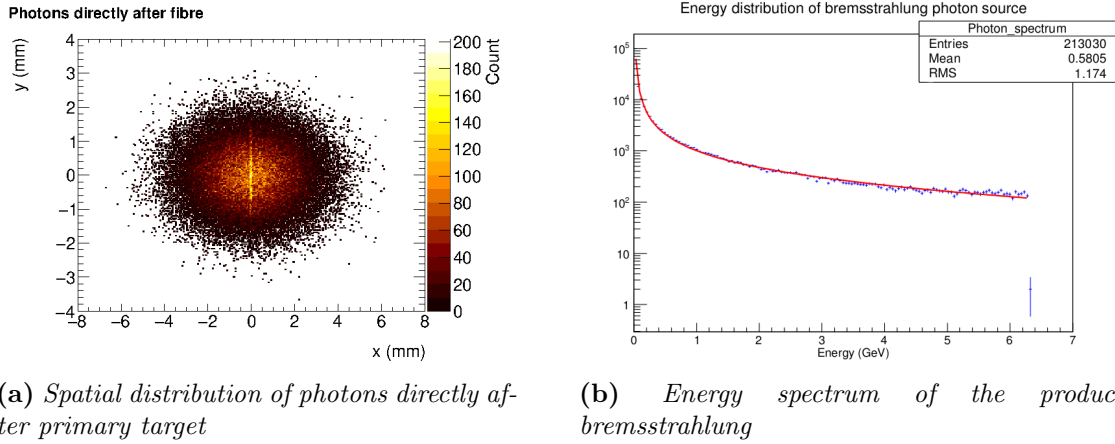


Figure 3: The bremsstrahlungsspectrum of an electron bunch hitting the carbon fibre which was used as a starting point for the simulations.

To reduce the amount of computer processing to be done, the main simulation uses a file with information from a previous simulation of the particle bunch hitting the primary target.[1] This file contains the photon energies and positions, which were used as the starting point for further simulations. The energy distribution of the bremsstrahlung photons can be seen in plot 3. Next to it is a scatterplot showing the spacial distribution of the photons directly after the fibre.

The test beam geometry was described in a gdm1 and a xml file, which were combined into an Linear Collider Detector Description (LCDD) file. This file, together with the result from the simulation of the beam hitting the primary target, formed the main input for the simulations. The result of the simulations with SLIC are stored in Linear Collider I/O (LCIO) files, which can be converted to ROOT files using Marlin, a software framework for processing LCIO files.[7]

3.1 Neutron production in shielding material

As the neutrons are mainly produced in the shielding material around the converter target, only the first part of the test beam geometry was simulated. The elements from the converter target on, were taken out of the geometry, allowing a quicker simulation. The simulation was performed for 10 DESY-II bunches hitting the primary target and using two different physics lists. Physics lists represent the physical laws in Geant4 simulations. The first physics list used, LCPHYS, is the default list for SLIC. Furthermore, a physics list optimised for hadron interactions was used, QGSP_BERT_HP.

3.2 Energy distribution of the final Test Beam using different converter plates

For the second part of the simulations each converter target was simulated at 6 different magnetic field strengths in the dipole magnet, so that 12 different simulations were performed. Each simulation was done for the full geometry of the test beam. The LCPHYS physics lists was used for all simulations and for each combination 200 bunches were simulated. Data for the copper converter plate of 5 mm from a previous simulation of test beam 21 [1] was used in addition to the results from the simulations performed for the Cu and the Al 3 mm converters, so in total data from 18 independent full simulations.

4 Results and discussion

4.1 Neutron Fluxes

In figure 4 the energy spectrum of the neutrons produced in the shielding materials can be seen. The rest mass is included in the energy value, so the spectrum only starts at 0.94 GeV. The results from the two physics lists agree well with each other, both in the energy spectrum and in the number of neutrons produced.

Energy of neutrons at creation

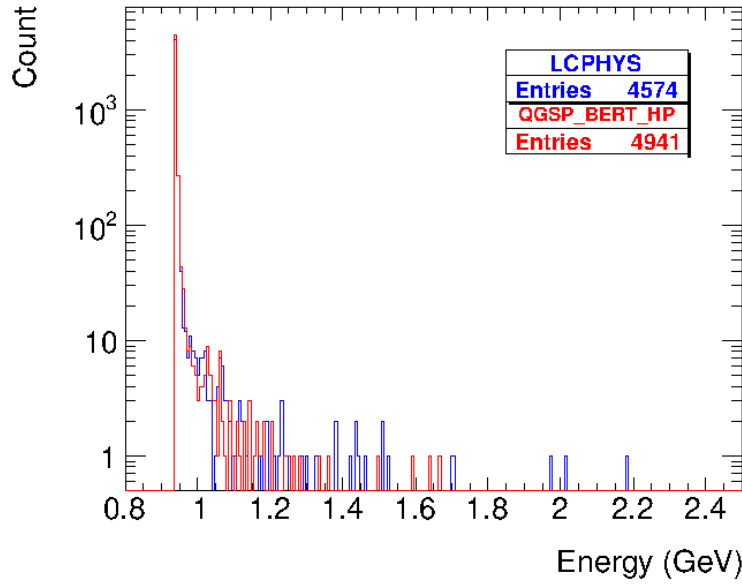


Figure 4: *Energy spectrum of neutrons produced in shielding material*

In figure 5 two scatterplots of the position of the neutrons directly after the first shielding is shown, where z-axis is the direction of propagation of the test beam. Here a difference between the results exists, as the results from the QGSP.BERT_HP show a distribution which is more concentrated around the z-axis. Both plots show a random distribution of neutrons in the x-y plane around the z-axis, which would be expected for random scattering and interaction processes.

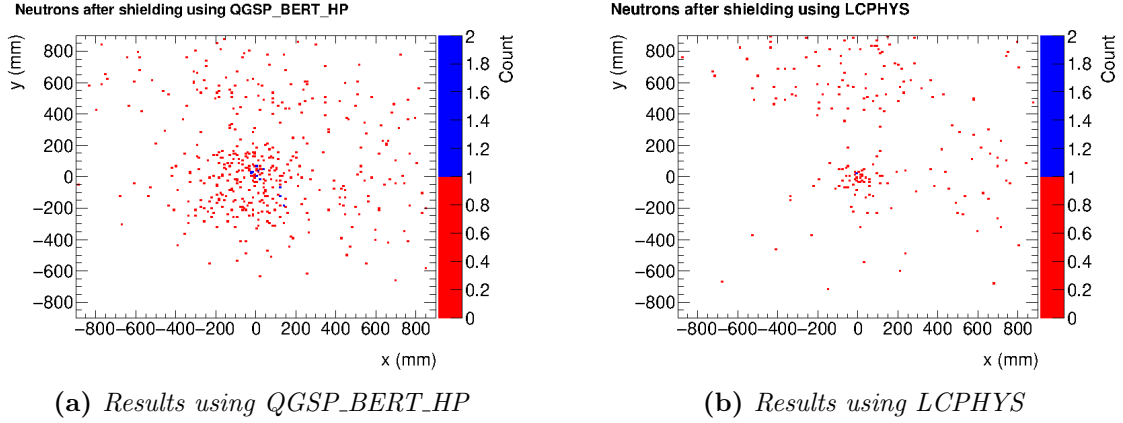


Figure 5: *Spatial distribution of neutrons directly after the shielding of the converter*

When considering both the energy spectrum and the spacial distribution, the physics lists give quite similar results. The simulations were done with relatively few particles,

only 10 bunches, so differences might become more or less distinct with a more extensive simulation.

The number of neutrons produced is relatively low and will not contribute significantly to activation of materials in the DESY-II tunnel. However, highly sensitive detectors such as scintillators can be damaged by neutrons. The neutron radiation should therefore be considered when doing measurements in the DESY-II tunnel.

4.2 Photon conversion efficiencies

To be able to compare the simulation results with old experimental results, a plot of the number of electrons in the final beam as a function of the mean electron energy was made.

For each simulation the energy distribution of the electrons directly after the final collimator in the test beam area was plotted and fitted with a double Gaussian, one Gaussian for the signal and one for the background. Using the mean value and the standard deviation of the signal Gaussian, the number of electrons directly after the final collimator with an energy within one standard deviation of the mean energy was found. An example of this fit can be seen in figure 6. The χ^2 value is for the double Gaussian, whereas the mean and sigma values are for the signal peak. The double Gaussian fits the data well, as demonstrated by the low χ^2 value of 1.99 for the fit in the plot. The other 17 fits, which can be found in the appendix, all have a χ^2 value under 3.5, most even under 2.

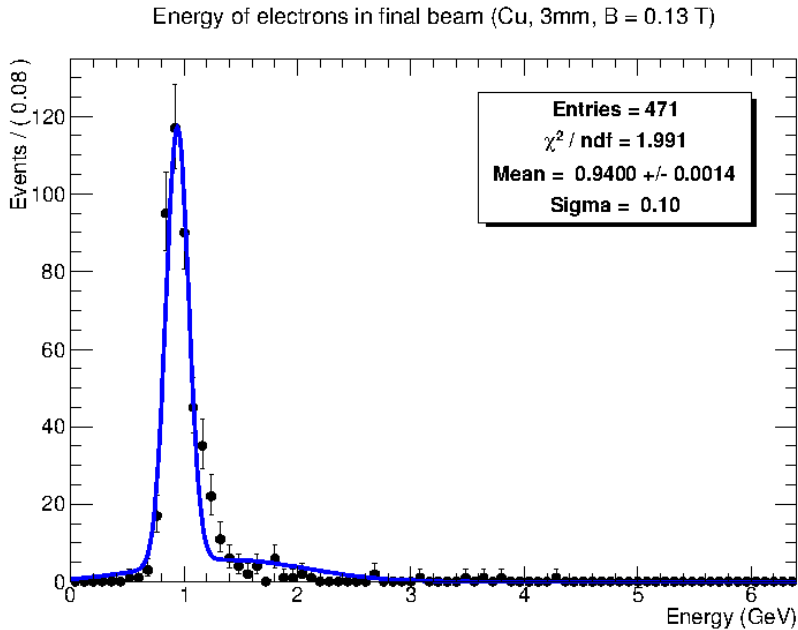


Figure 6: *Energy spectrum of final beam for the 3mm Cu target with the magnet at $B = 0.13$ T*

Using the number of electrons with the required energy and the mean energy value for each of the simulations, the plot in figure 7 was made. As expected the copper targets give the highest rates of electrons in the final beam, specifically the thicker copper target.

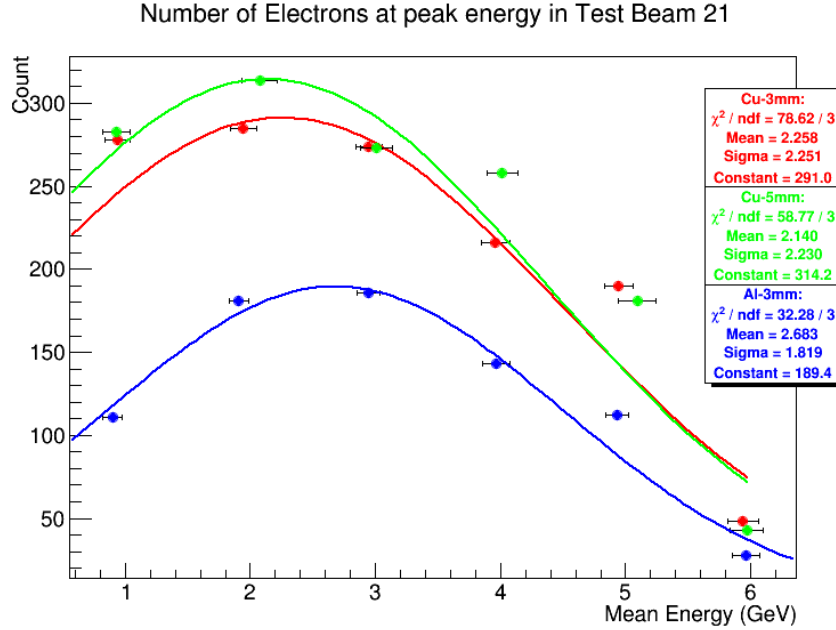


Figure 7: *Number of electrons with energy within one standard deviation of the mean energy at several mean energies for three different converter plates*

There is a peak particle rate between 2 and 3 GeV. From the bremsstrahlung spectrum alone, one would expect higher rates at 1 GeV. However, lower energy particles have a higher chance of interacting with the surrounding materials and therefore higher losses due to scattering are expected, explaining the lower particle rates at lower energies. The rate for the peak energy around 6 GeV is very low, which can be explained by considering the energy of the DESY-II beam bunch. The primary particles only have an energy of 6.3 GeV, so after 2 conversions and multiple collimations the number of particles produced at 6 GeV is significantly lower than at the lower energies. This can also be seen in the bremsstrahlung spectrum in figure 3, as the number of photons produced with high energy is much smaller than the number of photons at lower energies.

When looking at the experimental data in figure 1, a clear Gaussian distribution can be observed. The results from the simulation show a less distinct Gaussian distribution, but still have a similar shape.

The highest particle rate in the experimental data is at the same mean energy for all converters, but the peaks are shifted relative to each other for the simulated targets. This may depend on the fit, both of the primary energy plots and of the final plot. Furthermore, the statistics could be improved by doing further simulations, as only 200 bunches are simulated per magnet and converter configuration and exactly

the same bremsstrahlungsspectrum is used for every simulation. Due to transverse movement of the beam in the DESY-II ring the initial bremsstrahlungsspectrum might change constantly and cause a different energy spectrum of the final beam. To include this effect in the simulation, one would need multiple input files representing different bremsstrahlungsspectra.

5 Conclusions

The DESY-II test beam is an interesting subject for simulations due to the two conversion stages and effect of different secondary targets on the final test beam. Next to the secondary particles required for the final test beam, also neutrons are produced in the test beam line in the DESY-II tunnel. The neutrons, which are mainly produced in the shielding materials around the secondary target, can damage detectors and therefore these neutron fluxes should be considered when placing detectors in the DESY-II tunnel. Energy spectrum plots of single simulations show a clear peak in energy, as expected. Results from these plots were used for one final plot summarising the results of 18 simulations showing the dependency of the electron rate on the converter target used and the peak energy of the final beam.

The simulations of the test beam using different converter targets reproduce the experimental data quite well. The rates of final particles vary with material and thickness of the converter plate used and give higher rates for copper, with the highest rates for the thicker converter plate. When fitting the simulation results, a Gaussian shape could be used, though the experimental data shows a clearer Gaussian distribution. This could be caused by low statistics or by errors in the fitting of the primary energy plots.

It would be interesting to do further simulations for finding better converter plate materials, for example using tungsten. This could produce even higher rates in the final beam and give users more statistics for testing. Also further simulations to improve statistics could be useful, specifically with multiple input files with different bremsstrahlungsspectra.

Appendix

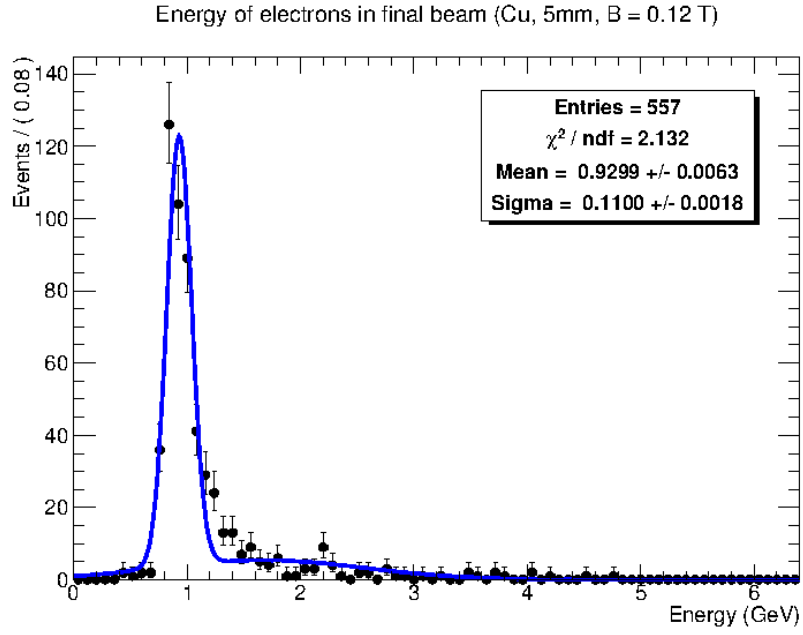


Figure A.1: Energy spectrum of final beam using 5mm Cu target with $\langle E \rangle = 1\text{ GeV}$

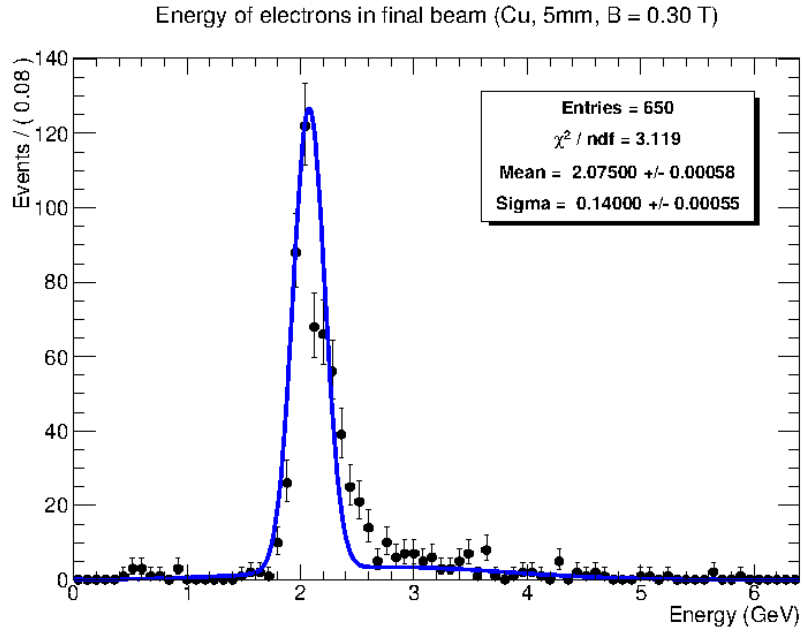


Figure A.2: Energy spectrum of final beam using 5mm Cu target with $\langle E \rangle = 2\text{ GeV}$

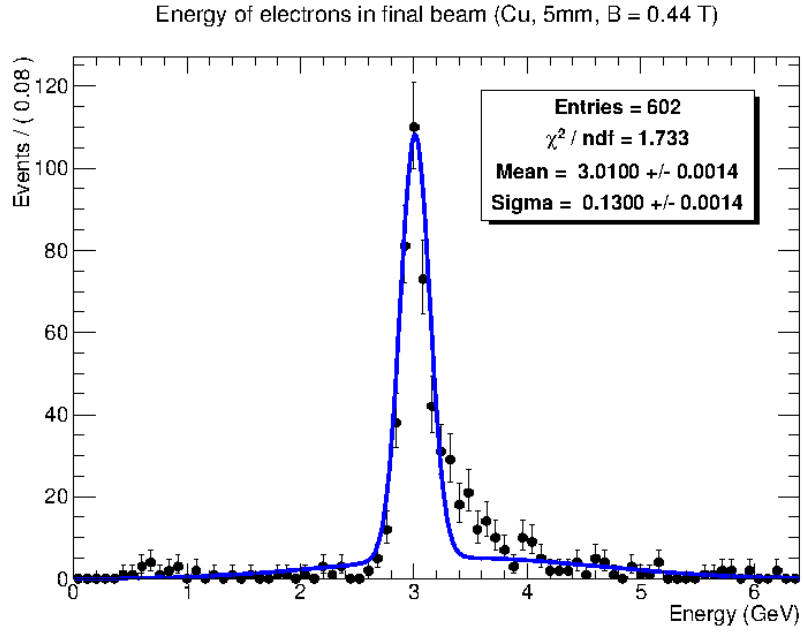


Figure A.3: *Energy spectrum of final beam using 5mm Cu target with $\langle E \rangle = 3$ GeV*

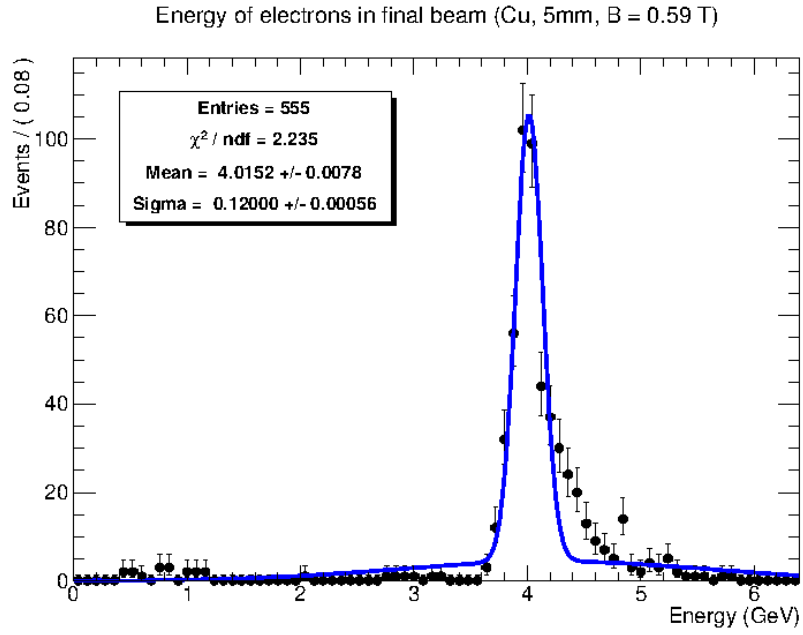


Figure A.4: *Energy spectrum of final beam using 5mm Cu target with $\langle E \rangle = 4$ GeV*

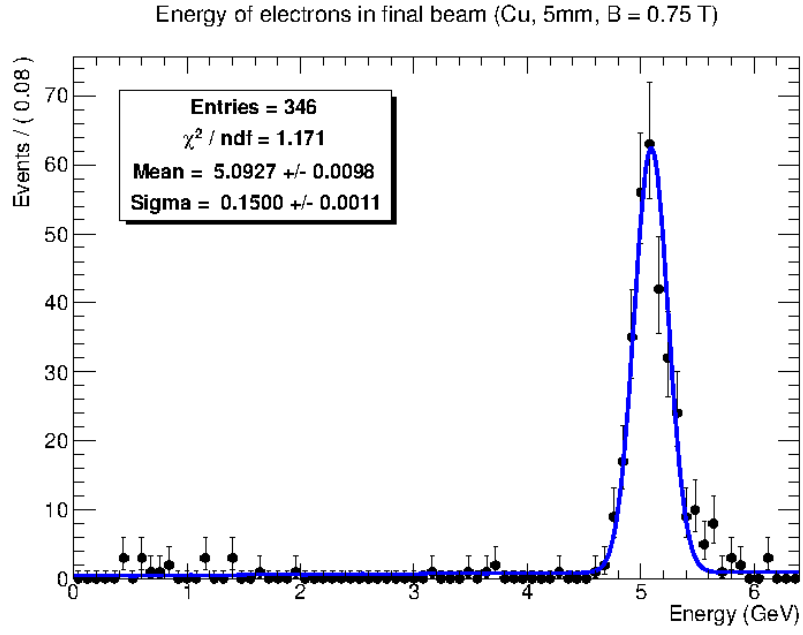


Figure A.5: Energy spectrum of final beam using 5mm Cu target with $\langle E \rangle = 5$ GeV

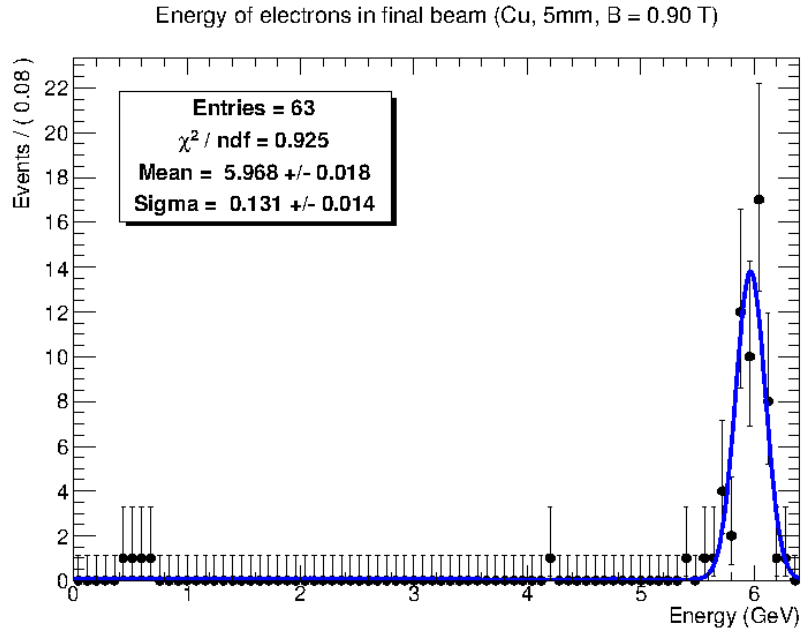


Figure A.6: Energy spectrum of final beam using 5mm Cu target with $\langle E \rangle = 6$ GeV

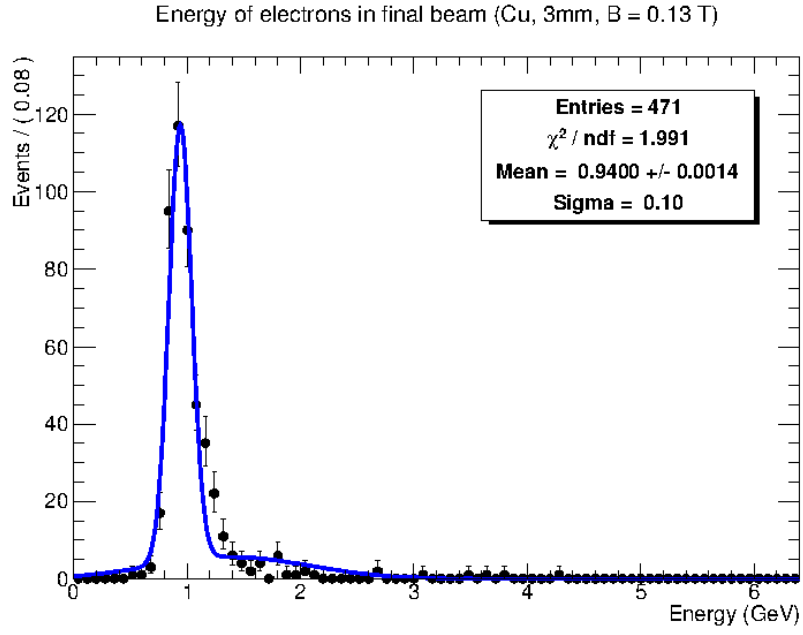


Figure A.7: Energy spectrum of final beam using 3mm Cu target with $\langle E \rangle = 1$ GeV

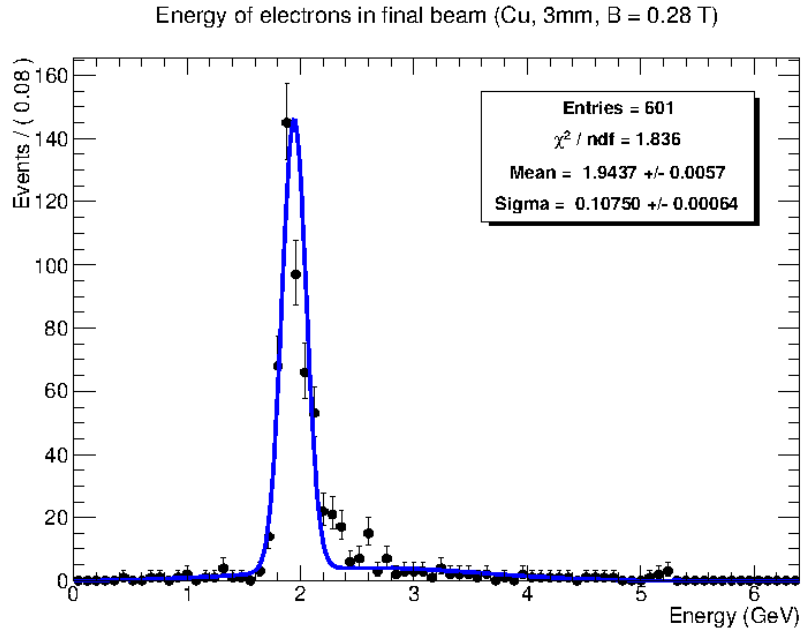


Figure A.8: Energy spectrum of final beam using 3mm Cu target with $\langle E \rangle = 2$ GeV

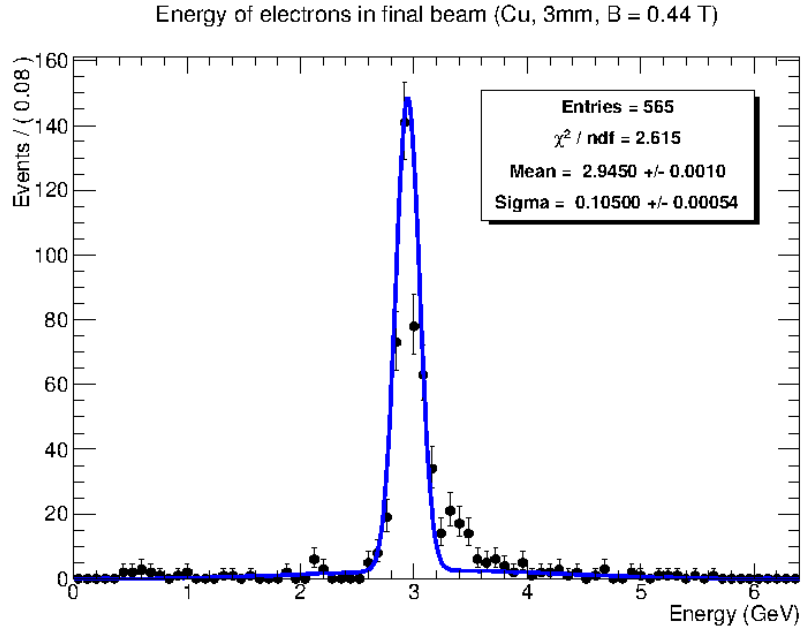


Figure A.9: *Energy spectrum of final beam using 3mm Cu target with $\langle E \rangle = 3$ GeV*

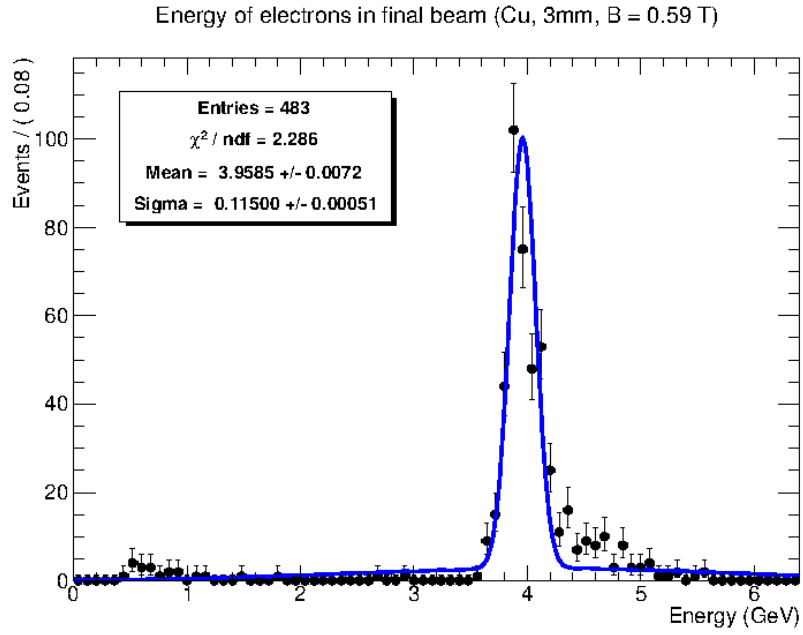


Figure A.10: *Energy spectrum of final beam using 3mm Cu target with $\langle E \rangle = 4$ GeV*

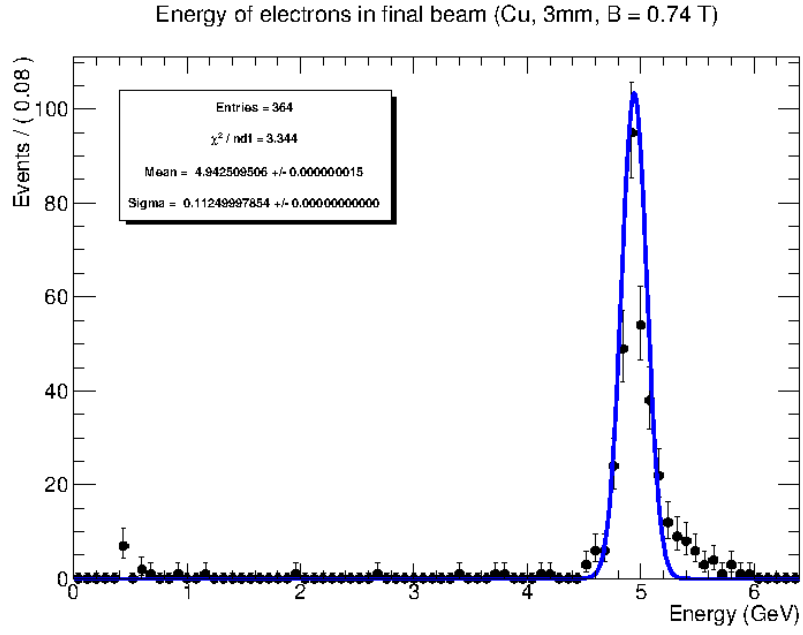


Figure A.11: *Energy spectrum of final beam using 3mm Cu target with $\langle E \rangle = 5$ GeV*

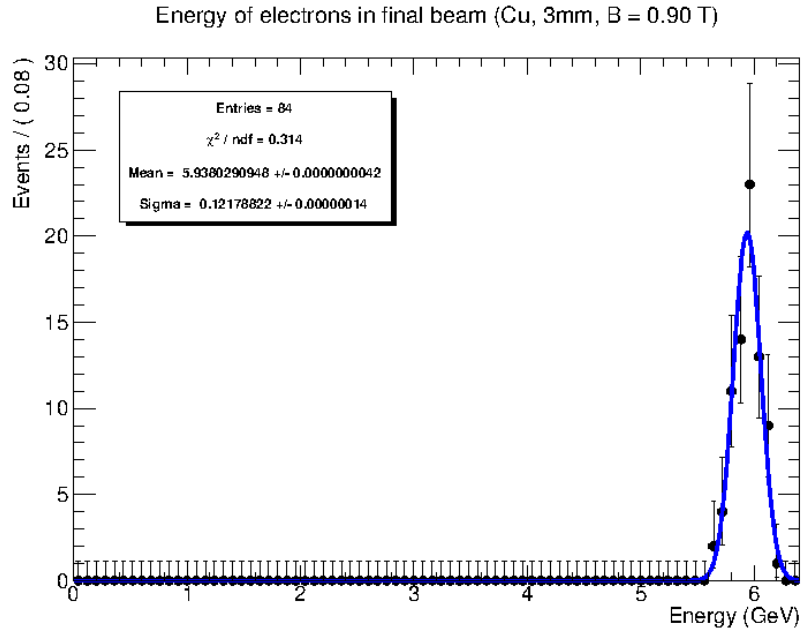


Figure A.12: *Energy spectrum of final beam using 3mm Cu target with $\langle E \rangle = 6$ GeV*

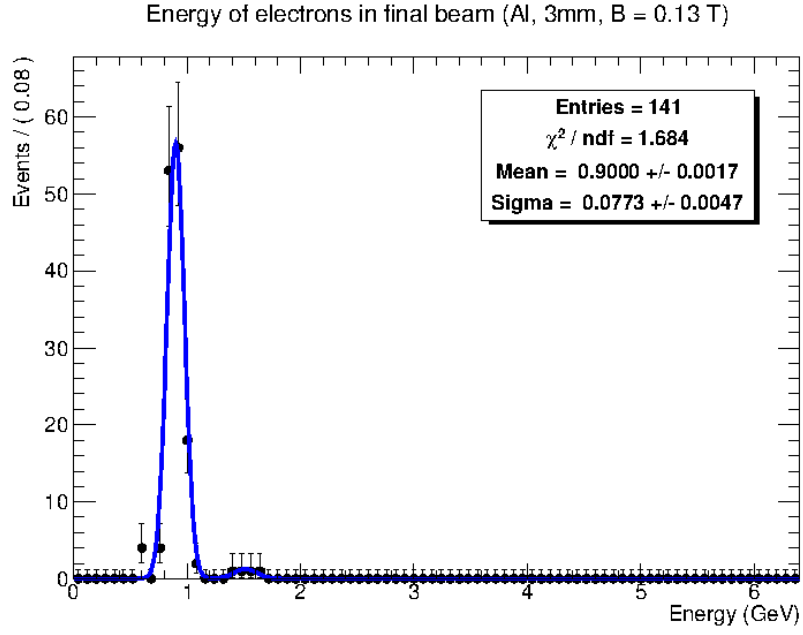


Figure A.13: *Energy spectrum of final beam using 3mm Al target with $\langle E \rangle = 1\text{ GeV}$*

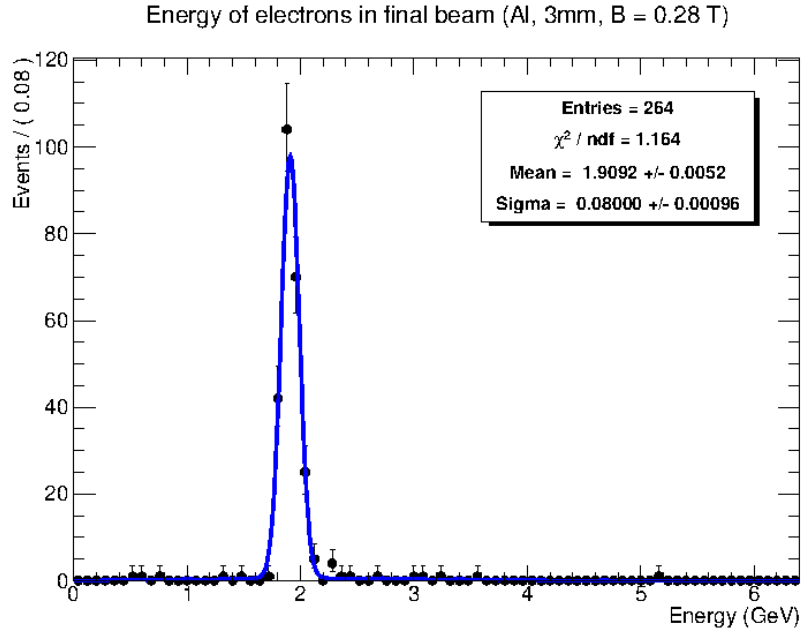


Figure A.14: *Energy spectrum of final beam using 3mm Al target with $\langle E \rangle = 2\text{ GeV}$*

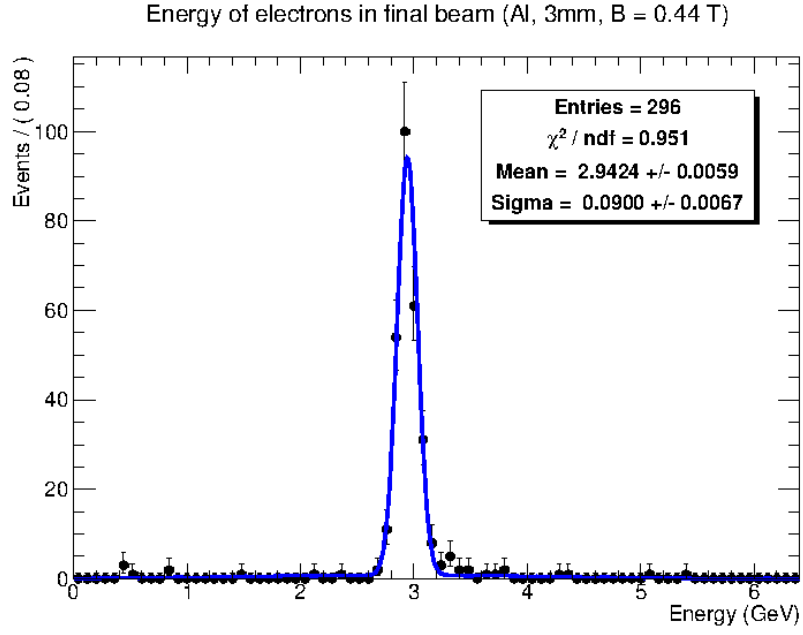


Figure A.15: *Energy spectrum of final beam using 3mm Al target with $\langle E \rangle = 3\text{ GeV}$*

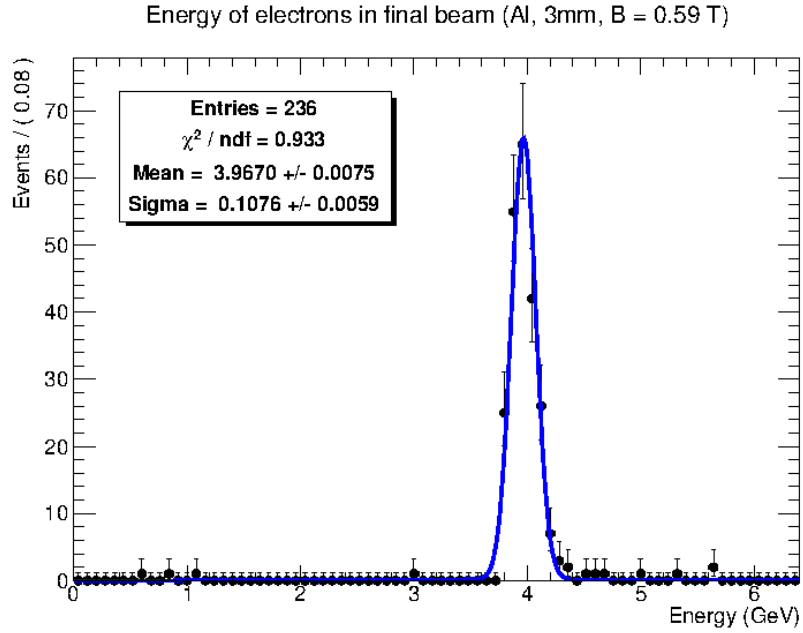


Figure A.16: *Energy spectrum of final beam using 3mm Al target with $\langle E \rangle = 4\text{ GeV}$*

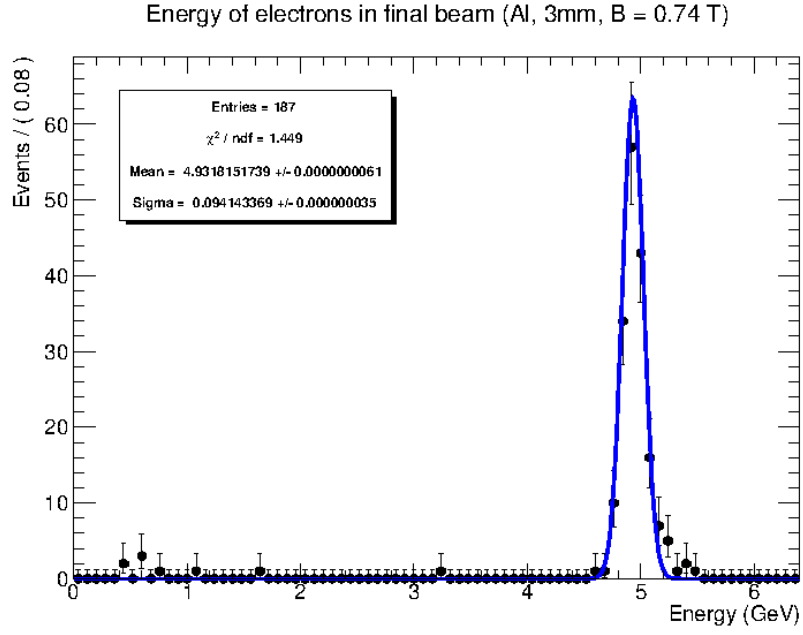


Figure A.17: *Energy spectrum of final beam using 3mm Al target with $\langle E \rangle = 5$ GeV*

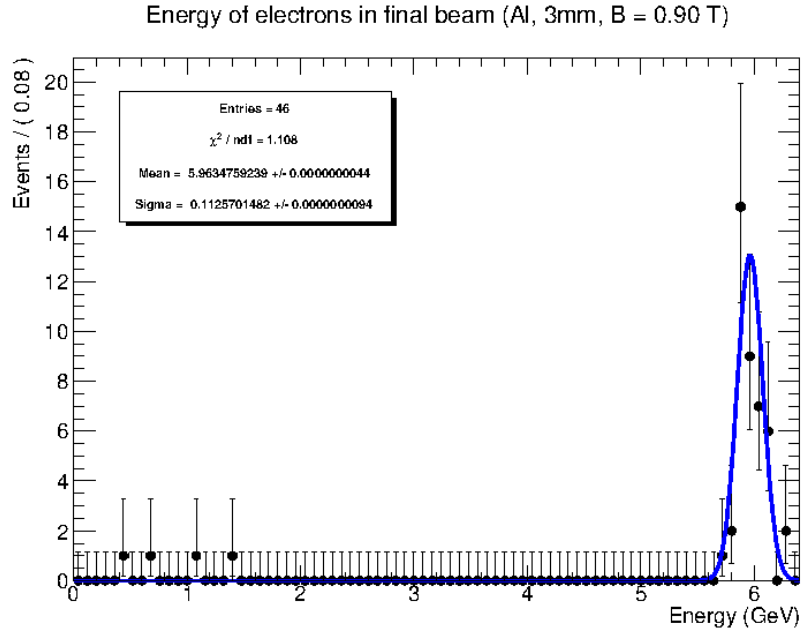


Figure A.18: *Energy spectrum of final beam using 3mm Al target with $\langle E \rangle = 6$ GeV*

Acknowledgments

I would like to thank my supervisors for first of all proposing this interesting project and then for all their help during the project. I learned very much and experienced how nice working in research can be. My summer at DESY in the ATLAS Group was great and I would also like to thank all members of the ATLAS Group for making me feel very welcome at DESY. Specifically I would like to thank Phillip Hamnett for his help with RooFit, without which fitting would have been much more complicated. Last but not least I would like to thank the DESY Summer Student Programme 2015 organisers for inviting me to DESY and enabling this summer project in the first place.

References

- [1] Schütz, Anne. *Simulation Of Particle Fluxes At The DESY-II Test Beam Facility*. Master's Thesis. Karlsruhe Institute of Technology, Karlsruhe, and DESY, Hamburg, 2015.
- [2] DESY. Test Beams At DESY, DESY II Description, Fig. 7 Rates Vs Momentum Beam Line 21. 2008. http://particle-physics.desy.de/test_beams_at_desy/desy_ii_description_status/index_ger.html Web. 27 Aug. 2015.
- [3] Povh, Bogdan. *Particles And Nuclei: An Introduction To The Physical Concepts*. 7th ed. Heidelberg: Springer, 2015. Web. 28 Aug. 2015.
- [4] Speth, Joseph, and Adriaan van der Woude. 'Giant Resonances In Nuclei'. *Reports on Progress in Physics* 44.7 (1981) Web. 28 Aug. 2015.
- [5] DESY-II parameters. Private communication with Heiko Ehrlichmann, DESY MDE, Leader of Machine-Division group for the DESY-II synchrotron accelerator
- [6] McCormick, Jeremy. 'SLIC FAQ - Linear Collider - SLAC Confluence'. <https://confluence.slac.stanford.edu/display/ilc/SLIC+FAQ> N.p., 2013. Web. 28 Aug. 2015.
- [7] 'Marlin'. http://ilcsoft.desy.de/portal/software_packages/marlin/ N.p. Web. 7 Sept. 2015